# Chapter 7
# Classical and Nonclassical Theories of Crystal Growth

**Jens-Petter Andreassen and Alison Emslie Lewis**

In this chapter, we discuss classical and nonclassical concepts of crystal growth that coexist in the literature as explanations for the formation of both mono- and polycrystalline particles, often of the same substances. Crystalline particles with intraparticle nanosized subunits, nanoparticulate surface features, and complex morphologies have led to the development of new nonclassical theories of crystal growth based on the aggregation of nanocrystals in solution. At the same time, similar morphologies are explained by monomer incorporation at conditions of stress incorporation, which results in nucleation at the growth front and accompanying branching at the nanoscale. The two mechanisms are differently affected by important process variables like supersaturation, temperature, or additives and are analyzed with respect to their capability of predicting crystal growth rates. A quantitative description of the formation kinetics of the solid phases is essential for the design and operation of industrial precipitation and crystallization processes and for the understanding of fundamental principles in material design and biomineralization processes. In this chapter, we emphasize the importance of supersaturation in order to account for the extensive nanoparticle formation required to build micron-sized particles by nano-aggregative growth, as well as the accompanying change in the population density.

J.-P. Andreassen (✉)
Department of chemical engineering, Norwegian university of science and technology (NTNU), Trondheim, Norway
e-mail: Jens-Petter.Andreassen@ntnu.no

A.E. Lewis
Department of chemical engineering, University of Cape Town, Cape Town, South Africa



A.E.S. Van Driessche et al. (eds.), *New Perspectives on Mineral Nucleation and Growth*,
DOI 10.1007/978-3-319-45669-0_7

## 7.1 Introduction

During the last decades, various nonclassical concepts of crystal growth have emerged in the scientific literature (Matijevic 1993; Cölfen and Antonietti 2008). They depart from the classical growth theories (Chernov 1984) by proposing that crystals, both mono- and polycrystalline, are produced by aggregation or assembly of nucleated nanocrystals, as opposed to integration of solute species into the crystal lattice surface. These novel concepts have received considerable attention and are now used extensively in the literature to analyze crystallization and precipitation phenomena in both nature and industry.

Classical mechanistic explanations of crystal growth have traditionally focused on explaining the microscopic features of the crystal surfaces and the integration of growth units leading to the development of faceted crystals. Derivation of the corresponding rate expressions, accompanied by experimental verification, has provided industrial practitioners with a tool to model and predict crystal morphology and size. Emerging fields in material technology, nanoparticle science, and biomineralization have introduced new experimental conditions and protocols, resulting in particle morphologies that are very often quite different from the expected equilibrium morphologies. Precipitation occurring at higher supersaturation and temperatures, often in combination with additives and templates, results in various examples of complex shapes and surface feature expressions that are not in accordance with the classical morphology predictions from an energy minimization viewpoint. The advancement of characterization techniques has opened up the ability to carry out more detailed studies of processes going on during nucleation, growth, and aggregation. New nonclassical concepts of crystal growth have been proposed as a consequence of this. Phase change kinetics by these alternative routes will be very different from what the classical theories predict. In this chapter, we present some of the dominant concepts of crystal growth and discuss the main differences between them, since the many different and often conflicting explanations presented in the literature make studying and analyzing the phenomena of precipitation a challenge.

The aim is to identify which investigations are required to resolve the seemingly conflicting descriptions in literature when it comes to determination and prediction of growth kinetics during precipitation. This is motivated by the need for a consistent description of crystal enlargement processes and the effect of the main operating parameters during industrial manufacture and separation of crystalline materials from solution.

## 7.2 Driving Force and Size Enlargement

Enlargement of crystalline particles in solution is traditionally described by two processes: crystal growth and agglomeration due to encounters between the growing crystals. In this classical picture, crystal growth is considered to progress by

attachment of monomeric growth units from solution. These solute species are the ions, molecules, or atoms which correspond to the primary constituents of the crystal lattice. The driving force for solute incorporation is the difference in their activity as solution species, $a$, and as incorporated in the solid, represented by the activity of solution in equilibrium with the solid, $a_{eq}$. The corresponding chemical potential difference, $\Delta\mu$, for a non-dissociating compound can be expressed as

$$\frac{\Delta\mu}{RT} = \ln\frac{a}{a_{\mathrm{eq}}} \tag{7.1}$$

leading to definition of the supersaturation ratio, $S_{\mathrm{a}}$

$$S_{\mathrm{a}} = \frac{a}{a_{\mathrm{eq}}} \tag{7.2}$$

For minerals and electrolyte crystals where each formula unit consists of a total number of $\nu$ ions, being the sum of $\nu_+$ cations and $\nu_-$ anions, the expression becomes

$$\frac{\Delta\mu}{RT} = \nu\ln\frac{a_{\pm}}{a_{\pm,\mathrm{eq}}} \tag{7.3}$$

where $a_{\pm}$ is the mean activity of the ionic species, resulting from the correction of the free concentration of ions, $c$, by the mean activity coefficient, $\gamma_{\pm}$. For crystals composed of two divalent ions, like $CaCO_3$, the corresponding activity-based supersaturation is thus

$$S_{\mathrm{a}} = \frac{a_{\pm}}{a_{\pm,\mathrm{eq}}} = \sqrt{\frac{c_{\mathrm{Ca}^{2+}}\cdot c_{\mathrm{CO_3}^{2-}}\cdot\gamma_{\pm}^2}{K_{\mathrm{sp,CaCO_3}}}} \tag{7.4}$$

In this classical picture, agglomeration is a rather rare event that will occur if the forces acting on the growing crystalline particles in solution cause them to approach each other closely enough so that a crystalline bridge develops resulting in a new stable particle. Hence in order for agglomeration to take place, crystal growth must occur during the time of contact, which also implies that the system must be supersaturated with respect to the crystallizing compound (Andreassen and Hounslow 2004). Investigations of agglomeration kinetics have concentrated on the contact brought about by shear forces in solution. In this context, agglomeration will depend on the collision rate of the growing crystals and an efficiency parameter that depends on the shape and contact point geometry and which also takes into account the disruptive hydrodynamic forces. In order for particles to be brought into contact by shear forces, their size needs to be in the micron meter range.

The recent new nonclassical theories challenge these ideas by claiming that also crystal growth is an aggregation process that can take place by assembly of nanosized crystalline particles by both oriented and non-oriented attachment,

operating at much smaller length scales. The attachment of particles must in this case be governed by very different forces (De Yoreo et al. 2015). The outcome of these assembly processes can be both poly- and monocrystalline, which in the latter case makes the end product indistinguishable from crystals growing according to a classical mechanism. For systems like calcium carbonate and barium sulfate, and many more, both classical and nonclassical explanations of crystal growth coexist in the recent literature. We will thus start by describing classical crystal growth and thereafter look into the newer theories and compare how the different conceptions explain prediction of morphology and the kinetics of the enlargement process.

## 7.3 Classical Crystal Growth by Monomers

### *7.3.1 At Low and Intermediate Supersaturation*

The incorporation of growth units from solution into the crystal lattice is a complicated process of attachment and detachment at active sites on the crystal surface. The attachment process involves desolvation of the monomers, adsorption onto the surface, and diffusion along the surface toward the active sites. Attachment at the active sites leads to advancement of steps over the surface. For the crystals to continue growing, new steps must be generated constantly. The dominant source of step formation varies with the supersaturation in the system. At driving forces lower than the critical value for surface nucleation, inherent dislocations in the crystal lattice are responsible for the presence of steps. Stacking faults lead to screw dislocations that represents a nonterminating step source since growth preserves the initial stacking fault of the lattice. Attachment along the screw dislocation step results in spiral growth and growth hillocks that eventually merge and cause the crystal face to propagate outwards. At a sufficient level of supersaturation, new steps are formed around two-dimensional islands that nucleate on the surface. The nucleation rate increases with supersaturation leading to a rough surface where integration of new units can potentially take place anywhere. The microscopic features of the surfaces growing by these two mechanisms of step generation can be observed by in situ AFM experiments as shown for the two examples of $BaSO_4$ and $CaCO_3$ in Fig. 7.1.

### *7.3.2 At High Supersaturation*

Despite that the surface features of spiral growth and 2-D nucleation growth can be observed at the microscopic level, crystal faces resulting from these mechanisms are macroscopically smooth and the crystals are dense. However, when further increasing the supersaturation, the interface becomes unstable due to a change from integration-controlled growth to mass-transfer-controlled growth, by diffusion from

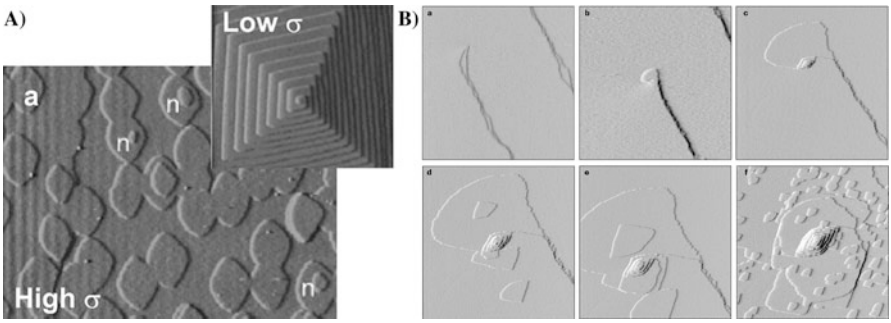


**Fig. 7.1** AFM images of crystal faces showing examples of spiral growth and growth hillocks at lower supersaturation and two-dimensional (2-D) nucleation islands at higher supersaturation for (**a**) calcite, $CaCO_3$ at two levels of supersaturation (σ corresponds to the left-hand side of Eq. 7.1) (Reproduced from De Yoreo and Vekilov (2003) with permission from the Mineral Society of America), and (**b**) barite, $BaSO_4$ – first five pictures in the panel is a growth sequence over 60 min for a supersaturation of $S_a^2 = 12$ (when $S_a$ is according to the definition in Eq. 7.4). In the last picture, the supersaturation has been increased, corresponding to $S_a^2 = 26$ (Reproduced from (Pina et al. 1998) with permission from Nature Publishing Group)

the surrounding bulk liquid. This transition (Fig. 7.2a) comes about when the surface turns rough and highly kinked due to extensive surface nucleation. Integration of new units is not rate limiting, and depending on the diffusion field around the crystal and the crystal morphology, certain edges and corners of the crystal will get access to solution of higher supersaturation. The consumption of supersaturation at these locations prevents growth of the central part of the crystal faces, and so-called "hopper" crystals develop. This elevation of the growth rate for certain parts of the crystal is self-enforcing, since the same edges, corners, or surface perturbations will access yet higher supersaturation levels and as a consequence dendritic growth starts to dominate. The crystal branches off in directions of higher supersaturation in an interplay dictated by the nature of the crystal lattice and the changing supersaturation profile from the surface into the bulk of the surrounding liquid. This branching is crystallographic, leading to a monocrystalline and usually symmetric object of complex shape. The shift in growth morphologies is a consequence of the change in growth regime and not the supersaturation itself. The supersaturation is merely responsible for introducing the diffusion limitation by increasing the monomer integration rate. This has been illustrated by similar morphology shifts due to diffusion limitations imposed by the surrounding medium, by performing mineral precipitation in hydrogels, relevant for biomineralization processes (Asenath-Smith et al. 2012).

The overall growth rate of crystals in solution is determined by the chemical affinity, the chemical potential difference between the solution and the crystal. The power law relationship shown in Eq. 7.5 is frequently used to relate the overall growth rate, $G$ [ms$^{-1}$], to the activity-based supersaturation ratio, $S_a$ (Eq. 7.4), and the solubility- and temperature-dependent growth rate constant, $k_g$. The growth order, $g$, signifies the mechanism of crystal growth. At low supersaturation, and

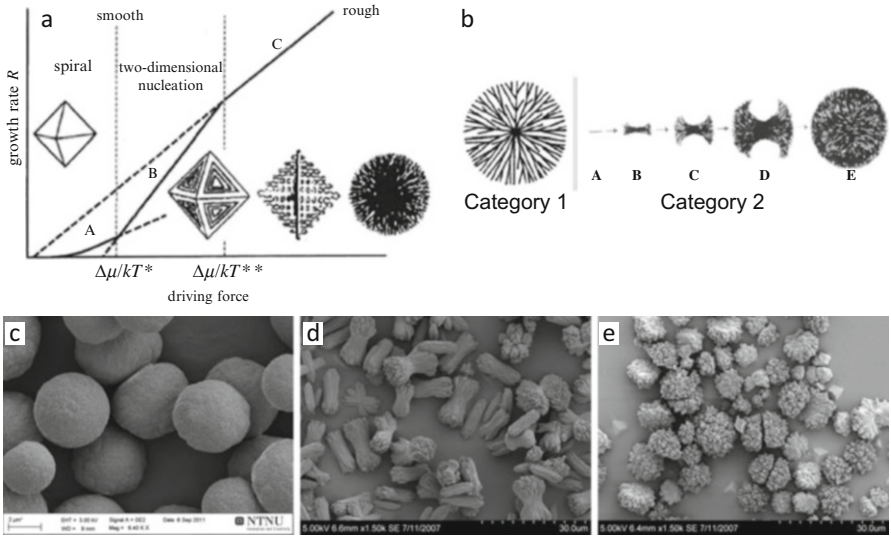


**Fig. 7.2** (**a**) Growth rate, crystal growth mechanisms (where A is spiral growth, B is growth by two-dimensional nucleation and C is rough growth) and corresponding morphology changes as a function of driving force for a hypothetical crystal bounded by {111} faces (Reproduced from Sunagawa (2005) with permission from Cambridge University Press). (**b**) Two categories of spherulitic growth: Category 1 describes multidirectional growth from a central nucleus, and category 2 describes growth front nucleation and resulting branching on the fast-growing tips of an elongated precursor crystal (A), leading to intermediate dumbbell morphologies (B-D) and potentially to a polycrystalline sphere (E) (Reproduced from Granasy et al. (2005) with permission from Cambridge University Press). (**c**) Category 1 vaterite spherulites grown in water at an initial supersaturation of $S_a = 5.7$ (with respect to vaterite) (Reproduced from Andreassen et al. (2012) with permission from RSC) (**d**) Intermediate-shaped category 2 spherulites grown at an initial $S_a$ (vaterite) = 3.8 in a mixture of ethylene glycol and water (90/10 %) and (**e**) nearly fully developed spherulites after 45 min when the initial supersaturation was increased to $S_a = 7.0$; the spherulites tend to break in two halves along the resulting equator (Reproduced from Andreassen et al. (2010) with permission from Elsevier)

provided that growth is dominated by simple, single sourced dislocation spirals, the value of $g$ is 2, resulting in the so-called parabolic growth law. When supersaturation is increased and 2-D nucleation starts to dominate, $g$ takes on higher numbers, evident of the exponential nature of the nucleation process. When the surface becomes rough and the growth rate is mass-transfer controlled, $g$ is equal to 1. Although the power law model is a simplified and averaged approach to the detailed crystal growth processes and composite mechanisms taking place on the surface of individual crystal faces (Teng et al. 2000), it has had success in the operation of industrial crystallization processes, by being used to adjust liquid phase parameters in order to control solid phase characteristics.

$$G = k_g(S_a - 1)^g \tag{7.5}$$

In contrast to the crystallographic branching that characterizes dendritic growth, a new branching mechanism starts to become operative at yet higher driving forces. Surface nucleation is no longer crystallographic and, as a result, the particle now becomes polycrystalline. This growth front nucleation will, as opposed to dendritic growth, often produce spherical space-filling structures, hence the term spherulitic growth. It has been a topic of numerous studies for well over a century, but is still not properly recognized in the precipitation literature. Spherulitic growth has been reported for various systems independent of the nature of the crystallizing compound. Molecular, atomic, and ionic crystals all grow by spherulitic growth, and although many of the studies are based on polymer crystallization and crystallization from viscous melts, it has been shown that neither large molecules, high viscosity, nor impurities are crucial for this mechanism (Beck and Andreassen 2010; Shtukenberg et al. 2012). Also crystals growing from pure aqueous solutions will produce spherulites when the conditions for internal stress accumulation, like high supersaturation, result in nucleation of new sub-individuals on the surface for the relaxation of this stress. The morphology will depend, firstly, on the progress of growth (supersaturation and branching frequency) and, secondly, on which of the two mechanisms of spherulitic growth in Fig. 7.2 that operates, which has been elegantly demonstrated by phase field modeling (Granasy et al. 2005). When growth front nucleation starts from a central nucleus, it results in isotropic type 1 spherulites, while type 2 spherulites are formed by branching on the two fast-growing faces of an elongated precursor, ultimately leading to polycrystalline spheres.

Both categories of spherulitic growth offer explanations of spherical polycrystalline particles without invoking an aggregation mechanism. Like for the other classical crystal growth mechanisms, the driving force $\Delta\mu$, is also a controlling factor for non-crystallographic branching, but the criteria for which type of spherulite that develops is not well known. As an example, both category 1 and 2 spherulites of the vaterite polymorph of calcium carbonate can be produced in solution at sufficiently high supersaturation (Fig. 7.1c–e). Category 1 spherulites grew by transformation from initially formed amorphous calcium carbonate (Andreassen 2005) in water, whereas category 2 spherulites developed in mixtures of ethylene glycol and water where the degree of branching was dependent on the initial supersaturation (Andreassen et al. 2010). Glycol reduces the growth rate of vaterite and allowed for a time-resolved observation of morphology development, but was not considered a prerequisite for this category of spherulitic growth. Category 2 spherulites of aragonite have been produced in water/ethanol mixtures (Sand et al. 2012) but also in aqueous solutions without additional solvents (Andreassen et al. 2012). The category 2 mechanism can offer an explanation for many other literature observations of sheaf of wheat and dumbbell morphologies that are described for crystalline mineral particles, like fluorapatite (Busch et al. 1999), $BaSO_4$ (Qi et al. 2000), and hematite (Sugimoto et al. 1993) but also in crystallization of higher-solubility compounds and from melts (Shtukenberg et al. 2012). The kinetic expression for spherulitic growth should reflect that this is an interface-controlled process driven by nucleation at the growth front and not diffusion controlled.

However, it has frequently been modeled as a diffusion problem, but this is related to the special conditions in many of the systems where spherulites are observed, i.e., high-viscosity metal or polymer melts where heat and mass transfer is limiting (Shtukenberg et al. 2012).

The mechanistic shifts and corresponding morphology predictions in classical crystal growth, from faceted monocrystals to surface-instability driven polycrystals, are explained with reference to the increasing supersaturation. Although there are some unresolved questions related to the phenomenon of non-crystallographic branching and the accompanying kinetic dependency on supersaturation, especially for growth in impurity-free low-viscosity media, the success of the classical monomer incorporation models has been their corresponding rate expressions that have been of great use to model industrial crystallization processes. The current alternative nonclassical concepts do not propose corresponding rate equations and do not necessarily obey the classical criterion related to the supersaturation dependence. They rather base their explanations on the colloidal stability of initially nucleated nanocrystals and how they may aggregate to create both mono- and polycrystalline structures.

## 7.4 Growth by Assembly of Precursor Crystals

A recent review (De Yoreo et al. 2015; see also Chap. 1 de Yoreo et al. 2017, this volume) presents a general concept of crystallization by particle attachment (CPA) by discussing attachment of a wider range of precursor particles, like oligomers, droplets, amorphous particles, or fully developed nanocrystals. We limit the following analysis to attachment and aggregation of prenucleated nanosized crystals.

Although polycrystallinity by growth of monomeric units can be explained by growth front nucleation, hardly any of the papers advocating an aggregation-based theory refer to such growth phenomena, indicating that it has been largely unknown in the field of mineral precipitation. However, it is of vital importance to understand whether growth is facilitated by particles nucleated in solution and transported to the crystal or if the resulting subunits nucleate and grow on the advancing crystal surface. In the former case, a high 3-D nucleation rate and hence a high supersaturation are required, as well as an efficient assembly or ordering principle, whereas in the latter case the degree of epitaxy and non-crystallographic branching during growth front nucleation is the determining factor for the level of polycrystallinity.

### *7.4.1 Spontaneous Precipitation Systems: Mesocrystals and Polycrystalline Particles*

Egon Matijevic (Matijevic 1993) was a pioneer in establishing an alternative interpretation of particle growth and proposed aggregation of nanosized crystals

as the mechanism responsible for the formation of polycrystalline micron-sized particles of various minerals. The underlying assumption was that an object that is spherical and polycrystalline can only be explained by assembly of already nucleated crystals, but other morphologies in the vast collection of "monodispersed" colloidal systems were also explained by a coagulation mechanism of nanoparticles. Ocaña et al. (Ocana et al. 1995) summarized some of the systems undergoing nano-aggregation and categorized the possible mechanisms as either undirectional or directional aggregation. Undirectional aggregation results in spherical particles, whereas ellipsoids, platelets, prisms, spheres, and rods could all be produced by directional aggregation, often assisted by additives.

Oriented attachment (OA) was demonstrated for a smaller assembly of nanoparticles some years later (Penn and Banfield 1999; see also Chap. 13 Penn et al. 2017, this volume) by hydrothermal treatment of 5 nm titania crystals (Fig. 7.3a). The particle size increased both by monomeric crystal growth and by assembly of up to ten individual crystals, a process that took place over several hours. When this oriented attachment process is non-perfect, it introduces dislocations in the resulting crystal (Penn and Banfield 1998), explaining how dislocations necessary for subsequent crystal growth can appear even though the initial nuclei are dislocation-free. Recent advances have allowed for direct observation of nanoparticle coalescence by high-resolution transmission electron microscopy using a fluid cell. In situ observations of platinum nanocrystals (Zheng et al. 2009) show that they grow by both monomer addition and particle-particle attachment events in the same order of numbers as that of the initial particles, illustrating that a few nanocrystals combine to make the new particles. This is an important growth

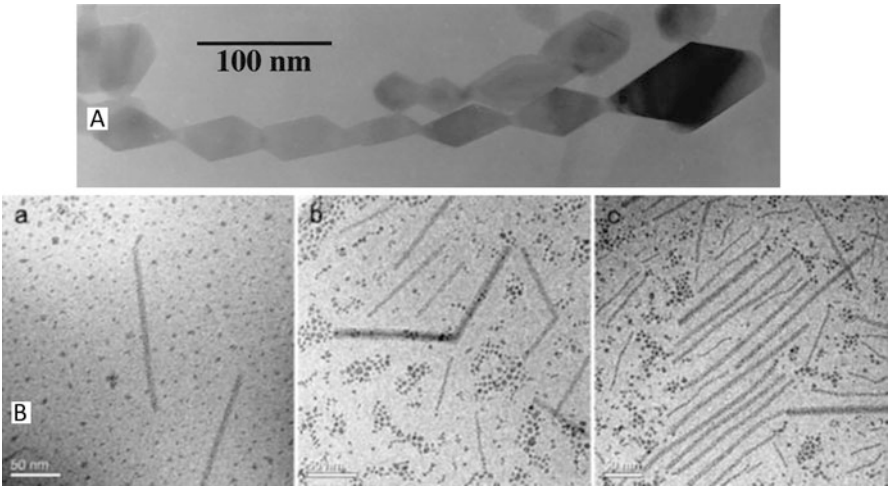


**Fig. 7.3** (**a**) TEM micrograph of a single crystal of anatase demonstrating oriented attachment of titania nanocrystals in 0.001 M HCl (Reproduced from Penn and Banfield (1999) with permission from Elsevier). (**b**) Cryo-TEM images of goethite mesocrystals developing by aging of a suspension of ferrihydrite nanocrystals at 80 °C, after (*a*) 5 days, (*b*) 10 days, and (*c*) 24 days (Reproduced from Yuwono et al. (2010) after permission from American Chemical Society)

trajectory to explain the nearly monodisperse particles resulting from an initially broad size distribution. The oriented attachment processes of iron oxyhydroxide nanoparticles observed in fluid cell TEM demonstrate how the particles rotate and interact until they find a perfect lattice match, and the attachment is followed by atom-by-atom addition. The translational and rotational accelerations show that direction-specific interactions drive the attachment, and the electrostatic field can promote these oriented attachment events (Li et al. 2012; Zhang et al. 2014; Nielsen et al. 2014).

The development of larger particles involving oriented attachment of a higher number of nanoparticles, in the orders of ten to hundreds, has been shown (Yuwono et al. 2010) by cryo-TEM monitoring of a suspension of ferrihydrite (Fig. 7.3b; see also Chap. 13 Penn et al. 2017, this volume). Over the course of several days, long thin mesocrystal assemblies of oriented goethite nanocrystals are developed by (1) self-assembly of primary nanocrystals, (2) crystallographic reorganization within the self-assemblies, and (3) conversion to oriented aggregates, which are new secondary crystals.

Directional aggregation has also been found to take place in the early process of gypsum precipitation (Van Driessche et al. 2012). The process started by formation of nanoparticles of the hemihydrate bassanite which after growth to nanorods of some 100 nm in length aggregated to needle-shaped particles which later transformed to the dihydrate gypsum. This oriented aggregation of bassanite was explained by an increase in the enthalpy with decreasing surface area, favoring aggregation over crystal growth.

Along with, and often based on, these demonstrations of crystal growth by oriented attachment, a significant number of studies in the recent literature have extended the argument to conclude that also larger micron-sized particles, both monocrystalline (Fig. 7.4) mesocrystals (Cölfen and Antonietti 2005; see also

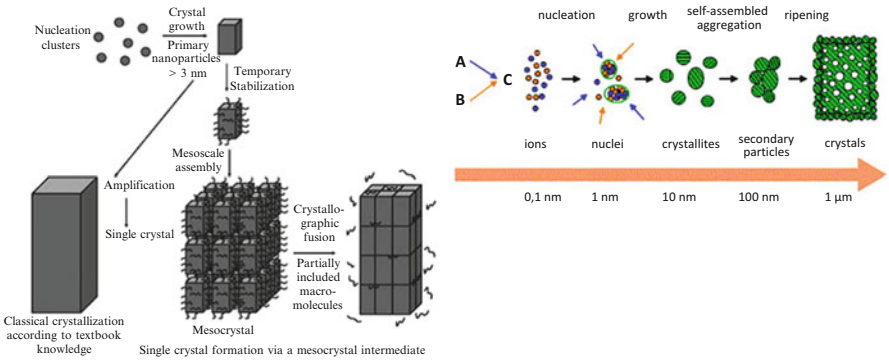


**Fig. 7.4** Aggregation schemes for monocrystalline particles in solution, *left*, assisted by macromolecules resulting in mesocrystals (Reproduced from Cölfen and Antonietti (2005) after permission from John Wiley and Sons) and, to the *right*, self-assembled aggregation in the absence of additives leading to porosity in the final crystals (Reprinted from Judat and Kind (2004) after permission from Elsevier)

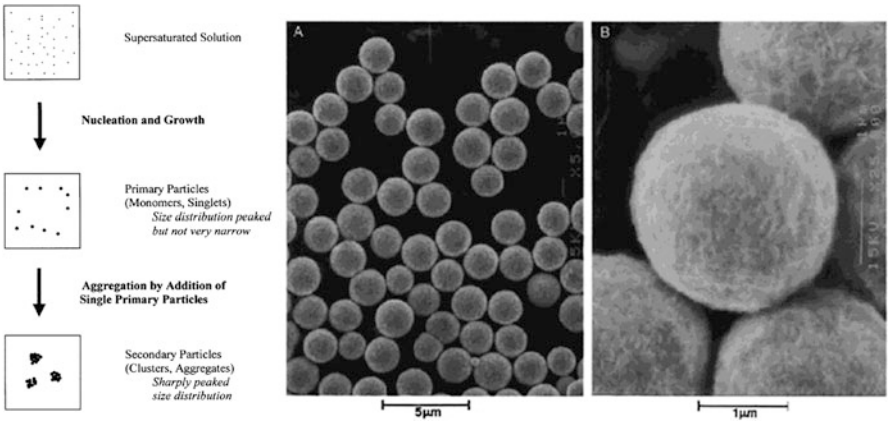


**Fig. 7.5** Aggregation scheme (to the *left*) illustrating how growth of monodisperse polycrystalline secondary particles of gold (by reduction of auric acid) in solution (micrograph *A* and *B*) occurs by addition of primary particles to secondary particles, to ensure a sharply peaked particle size distribution (Reproduced from Park et al. (2001) with permission from American Chemical Society)

Chap. 8 Rao and Cölfen 2017, this volume) and polycrystalline particles (Fig. 7.5), are formed by assembly mechanisms, suggesting that aggregation of nanocrystals is a universal mechanism for growth of crystalline particles. However, many orders of magnitude, higher number of primary nanocrystals and a highly efficient assembly mechanism, are required to account for these rapidly formed large micron-sized particles. Kind et al. (Judat and Kind 2004) used cryo-TEM to study shock-frozen samples from the rapid precipitation of $BaSO_4$ in a T-mixer arrangement and concluded that the internal porosity of the particles was a consequence of highly ordered aggregation of nanoparticles formed in the beginning of the process (Fig. 7.4). A similar evaluation of copper oxalate precipitation (Soare et al. 2006) discussed how the high ionic strength due to high concentration during nucleation would lead to aggregation of the nuclei, by suppression of the electric double layer and accompanying low colloidal stability. This initial random aggregation resulted in a core of randomly oriented primary particles whereas the outer aligned crystallites were explained by directional aggregation due to lower ionic strength at lower supersaturation later on in the growth process.

Calcium carbonate precipitation of both mono- and polycrystalline particles, both in the absence and presence of additives, is frequently explained as a result of non-classical crystal growth based on observations of intraparticle subunit structure and nanoparticle surface features. The argument of aggregation of nanosized crystals has been used to explain both polycrystalline spherical particles and monocrystalline hexagonal particles of vaterite. In the case of polycrystalline particles, aggregation is not oriented, but for the formation of hexagonal plates (Xu et al. 2006), additives in the system are said to be necessary to aid the assembly process, following a similar principle as described in Fig. 7.4. By contrast, it has been shown (Andreassen et al.

2012) that the morphologies of calcium carbonate that are explained as a result of modulating additives can in fact also be produced in the absence of any additives, by simply controlling the value of the activity-based supersaturation, $S_a$ (Eq. 7.4). It was concluded that calcium carbonate in this case forms by a classical growth mechanisms, since the supersaturation, $S_a$, is too low for the extensive nucleation required to supply an attachment process with the necessary primary crystalline particles.

Peak broadening in Powder XRD is widely used to support a nano-aggregation mechanism and the nanoparticle size is estimated by the Scherrer equation. The resulting size determination of the nano-domains tends to result in a range of 20–50 nm, irrespective of the mineral in question. Assuming that the final micron-sized particles would be constructed by aggregation of 20 nm particles in a space-filling structure, the number of primary crystals required for each final particle is in the order of $10^8$ (Andreassen 2005). Nucleation of such a high number of primary crystals, or building blocks, would require a substantial supersaturation, and their presence should be easily detectable in solution by in situ or cryo-TEM or even in dry samples separated from the solution during the 5-min growth period. In this case, the vaterite spheres were growing at a moderate supersaturation dictated by the transformation of amorphous calcium carbonate, and as a result, it was concluded that spherulitic growth was the operating mechanism and not aggregation of nucleated precursor crystals. When polycrystalline spheres of vaterite were seeded to systems of constant supersaturation well below the nucleation threshold, the particles grew by incorporation of ions from solution, constantly creating surface units that varied in size with the applied level of supersaturation (Andreassen et al. 2012), as predicted by the dependency of branching on the thermodynamic driving force (Shtukenberg et al. 2012). In a recent critical analysis of monocrystalline calcite mesocrystals precipitated in the presence of polymers (Kim et al. 2014), it was shown that the use of the Scherrer equation to infer information about primary building blocks is not valid and that the main source of the peak broadening was substantial strain in the crystal lattice which occurred when the crystals were grown in the presence of additives. In addition, the high surface area due to the nanoparticulate surface features could be fully explained as a consequence of the additive action on crystal growth in a classical sense. In a recent investigation, a polycrystalline vaterite biomineral (Pokroy et al. 2015) was also suggested to form from solution by ion-by-ion spherulitic growth, as opposed to nano-aggregation, due to 0 and 30° angle spreads and no interfacial organic layers between adjacent crystals. Other biomineralization examples where spherulitic growth has been shown is in the formation of earthworm granules (Hodson et al. 2015) and to infer information about microbial activity responsible for the formation of dolomite rock where some organisms make spherulitic Ca-Mg carbonate by increasing the supersaturation levels locally (McKenzie and Vasconcelos 2009).

In the current literature that uses the argument of aggregation of nanosized crystals, the total number of nanoparticles required and the reduction in numbers due to aggregation is normally not part of the analysis when attachment processes are discussed. However, in the classical industrial crystallization literature, it is essential to show that there has been a reduction in the number of crystals in order to

demonstrate that aggregation has taken place. A population balance analysis offers a consistent accounting tool to distinguish between particle enlargement by growth and by aggregation, and this has traditionally been applied for the agglomeration of larger crystals growing by classical crystal growth (Andreassen and Hounslow 2004; Costodes et al. 2006).

When it comes to the nonclassical growth mechanisms, only a few attempts have been made to quantify the kinetics of growth. Early attempts (Dirksen et al. 1990) to use a population balance approach to analyze aggregative growth of copper oxalate were performed, motivated by the morphology of the final particles. However, in order to explain the fairly monodisperse population of final particles from smaller crystals, it had to be assumed that aggregation takes place only by allowing nuclei to combine with larger particles, not by nuclei-nuclei or aggregate-aggregate events. A similar assumption was made to explain the rapid formation (10 s) of spherical micron-sized polycrystalline gold particles shown in Fig. 7.5 (Park et al. 2001). In order to account for the size selection leading to the final particles, the proposed aggregation units of 40 nm were assumed to only attach to secondary particles, which is not in accordance with later observations of single-single particle aggregation in liquid cell TEM (Zheng et al. 2009). However, the average secondary particle size predicted was smaller than the experimental values and the distribution was too narrow. In a later refined model (Libert et al. 2003) based on the synthesis of uniform cadmium sulfide particles, a new adjustable parameter was introduced. The number of primary particles in a typical secondary particle was estimated to be $2 \cdot 10^6$, but instead of allowing only for attachment of singlets to secondary particles, the experimental results were better explained by allowing cluster-to-cluster aggregation of secondary particles containing up to approximately 25 primary particles. These findings have not been verified by experiments. But this should be relatively uncomplicated, since such high numbers of particles in different states of aggregation should be clearly visible in both SEM and TEM.

### *7.4.2 Superparticles by Controlled Assembly of Nanosized Seed Crystals*

Another class of superstructures reported over the last decade could possibly shed some light on the previous discussion. Superparticles are based on the assembly of pre-made nanoparticles, made possible by the recent advances in nanoparticle manufacture. Superparticles can be grown from solution, where nanocrystals that are initially well dispersed can be brought together in larger particles resulting in a well-defined superlattice structure. As opposed to the spontaneous formation of meso- and polycrystals, precursor nanoparticles of well-controlled size and shape are fabricated in a separate step before the assembly principle is initiated. Bai et al. (Bai et al. 2007) produced colloidal spheres based on oil-in-water emulsions where the precursor crystals are functionalized with a surfactant and dispersed in the oil phase, which is subsequently removed by evaporation. Hence, the particle

size is a result of the nanocrystal concentration in the droplets as well as the emulsification process. For the assembly of 6.9 nm $BaCrO_4$ nanocrystals, the center-to-center distance inside the superparticles is 9.1 nm, which quantifies the TEM-observed interparticle gap to be 2.2 nm, caused by the presence of ligand molecules. This means that the nanocrystals kept their individual character and did not sinter into larger units despite prolonged heat treatment. The same was observed for nanoparticle micelles (Zhuang et al. 2008) that were dispersible in aqueous solution due to hydrophobic van der Waals interactions between the $Fe_3O_4$ nanoparticle ligands (oleic acid) and hydrocarbon chain of the surfactant (DTAB). By adding the nanoparticle-micelle solution to glycol, the micelles decomposed due to the loss of DTAB, and the $Fe_3O_4$ nanoparticles were then assembled due to solvophobic interactions between the nanoparticle ligands and glycol. The success and rate of the assembly was controlled by this solvophobic interaction by varying the amount of the surfactant, whereas CTAB prevented the assembly from taking place due to the lower solubility in glycol thereby preventing the solvophobic assembly. With DTAB, the rate of superparticle formation was generally fast and led initially to amorphous assemblies that only crystallized upon annealing. However, the individual nanocrystals were still separated within the superparticle crystal.

Assembly principles can also be applied for nanoparticles of opposite charge where the driving force for the aggregation process is governed by electrostatic forces. Kalsin et al. (Kalsin et al. 2006) prepared silver and gold NPs carrying positively and negatively alkane thiols, respectively. Both NP populations were stable separately, but when brought into contact, they eventually combined to superparticles, once the size distributions of the individual populations were appropriately tuned. Micron-sized supracrystals displaying the individual NP "ions" in a sphalerite structure were produced, but the assembly was occasionally unsuccessful producing a population of the individual NPs, or resulting in amorphous structures if the spread of the seed size distribution was less than optimal.

Based on the particle engineering principles described above, it seems clear that nanoparticles will assemble only once the conditions in terms of destabilization or association are realized at the right time and rate. This relies on separating the stages of nanoparticle formation and the subsequent formation of superparticle structures. In this respect, it differs significantly from the proposed formation mechanism of micron-sized mesocrystals and polycrystals which rely on nucleation of the sufficient number of nanocrystal building blocks in situ, a highly efficient assembly principle and mechanisms for removal of interparticle polymeric additives.

## 7.5 Outlook

The kinetics of crystal growth has a pivotal role in running processes for the design of particle products or for the prevention and inhibition of crystalline deposits. For that purpose, classical crystal growth has been successful in relating the chemical potential and temperature of the crystallizing medium to the rate of solid formation. The alternative aggregative growth concepts do not provide the same predictive

capability. This outlook summarizes the arguments of the above discussion and aims at recommending investigations that are required to resolve the current situation of two coexisting growth theories.

It has been demonstrated by in situ investigations in liquid cell TEM that a smaller number of nanocrystals will aggregate after nucleation and that this is important for the development of the nanoparticle size distribution and for development of dislocations. However, there is a large gap between these observations and the numbers required for the proposed extensive aggregation of nanocrystals responsible for the construction of larger micron-sized mesocrystals and polycrystalline particles, which can be in the order of $10^6$–$10^8$ primary crystals in each resulting secondary particle. The presence of such a high number of primary particles during an assembly process that goes on over a time period of seconds to minutes should also be easily identified in time-resolved TEM or cryo-TEM investigations, since the size of the building blocks is well within the detection limit of the microscopes.

The material balance is a classical tool that accounts for all species entering and leaving a system. The population balance method uses a number balancing approach in a similar way, to make sure that all particles in a process are accounted for and to ensure that number continuity is preserved. This is essential in order to prove that aggregation is taking place and to establish rate expressions for aggregation processes. Unlike classical crystal growth, only a few attempts have been performed to quantify precipitation rates in the case of nano-aggregative growth based on a population balance approach with varying and contradicting assumptions regarding aggregation events between primary particles and already formed assemblies. For formation of micron-sized particles based on nanocrystal assembly, the reduction in numbers should be accounted for in order to establish the mechanisms and kinetics of these growth processes.

Although variations in the free energy landscape and the surface energy can contribute to lower the critical free energy and hence change the pathway of the crystallization process, a significant reduction in the free energy due to increased supersaturation is still required to give the high nucleation rate of crystals necessary to provide the building blocks needed for the particle-based growth process. Hence, assembly-based growth of micron-sized particles from nanocrystals should only be possible in systems that are characterized by high supersaturation levels, unless a high nucleation rate is justified by other explanations. Future studies should be performed at quantified and varying levels of the supersaturation to establish that the nucleation rate is sufficient for the required number of nanocrystals. The effect of supersaturation on the aggregation mechanism must also be analyzed in order for nonclassical crystal growth to offer the same predictions as classical crystal growth when it comes to quantifying particle enlargement rates.

Due to the limited number of in situ observations at sufficiently high resolution, most of the evidence of nanocrystal aggregation is relying on observations of particles after completion of the formation pathway. However, many of the same features used to support an aggregation mechanism, like branched morphologies and nanosized surface units, can also be explained by far from equilibrium dendritic and spherulitic growth. It has been shown that diffraction line broadening is not evident of growth by aggregation, since lattice strain during classical growth can

give the same result. Classical growth by fast monomer incorporation can lead to strain development which leads to growth front nucleation and ultimately to non-crystallographic branching by increasing the supersaturation. Future investigations should thus analyze how classical growth mechanisms influenced by additives or running at high driving force can explain porosity and polycrystallinity. Dendritic and spherulitic growth can explain monocrystalline nonequilibrium particle morphologies and polycrystalline particles. However, spherulitic growth from solution is not well understood in terms of the kinetics of growth front nucleation, especially regarding the effect of temperature and driving force on the branching process. In the same way, as external morphology observations cannot be used to support a mechanism of nano-aggregation, it is also not a sufficient evidence to conclude on dendritic or spherulitic growth, and future mineralization studies should thus analyze the results in the framework of both concepts.

Attachment by rearrangement and lattice matching by rotation has been demonstrated for smaller ensembles of nanoparticles. Are these assembly mechanisms efficient enough for the aggregation of millions of nanocrystals on a timescale of seconds or minutes? The forces involved are not well understood, but, from the deliberate aggregation studies to design superparticles based on prefabricated nanoparticles, it becomes evident that aggregation is not trivial and association principles need to be finely tuned in order to result in assembly. Destabilization of the electric double layer and accompanying collisions due to Brownian motion is frequently used to explain the efficiency of aggregation. This hypothesis can be tested by manipulating the ionic strength of initially dispersed nanoparticles.

Since the assembly mechanisms involve highly specific aggregation of similarly shaped nanocrystals, especially in the case of directional growth, it should also be possible to prevent this assembly by steric hindrance with appropriate additives. This could provide proof that the driving force is sufficient for extensive nanoparticle generation, and at the same time, it can provide an efficient route to produce nanoparticles of various materials.

In order to resolve the current situation of two coexisting growth theories and the accompanying uncertainties when it comes to the kinetic predictions, more research is required. These future investigations should consider both nonclassical and classical mechanisms of crystal growth and in a systematic way compare evidence required to discriminate between them. Analyses of industrial precipitation processes depend on it, but the same fundamental questions also apply for minerals precipitating in natural processes.

## References

Andreassen JP (2005) Formation mechanism and morphology in precipitation of vaterite – nano aggregation or crystal growth? J Cryst Growth 274:256–264

Andreassen JP, Hounslow MJ (2004) Growth and aggregation of vaterite in seeded-batch experiments. Aiche J 50:2772–2782

Andreassen JP, Flaten EM, Beck R, Lewis AE (2010) Investigations of spherulitic growth in industrial crystallization. Chem Eng Res Des 88:1163–1168

Andreassen JP, Beck R, Nergaard M (2012) Biomimetic type morphologies of calcium carbonate grown in absence of additives. Faraday Discuss 159:247–261

Asenath-Smith E, Li H, Keene EC, Seh ZW, Estroff LA (2012) Crystal growth of calcium carbonate in hydrogels as a model of biomineralization. Adv Funct Mater 22:2891–2914

Bai F, Wang D, Huo Z, Chen W, Liu L, Liang X, Chen C, Wang X, Peng Q, Li Y (2007) A versatile bottom-up assembly approach to colloidal spheres from nanocrystals. Angew Chem Int Ed 46:6650–6653

Beck R, Andreassen JP (2010) Spherulitic growth of calcium carbonate. Cryst Growth Des 10:2934–2947

Busch S, Dolhaine H, Duchesne A, Heinz S, Hochrein O, Laeri F, Podebrad O, Vietze U, Weiland T, Kniep R (1999) Biomimetic morphogenesis of fluorapatite-gelatin composites: fractal growth, the question of intrinsic electric fields, core/shell assemblies, hollow spheres and reorganization of denatured collagen. Eur J Inorg Chem 1999:1643–1653

Chernov AA (1984) Modern crystallography III: crystal growth. Springer, Berlin

Cölfen H, Antonietti M (2005) Mesocrystals: inorganic superstructures made by highly parallel crystallization and controlled alignment. Angew Chem Int Ed 44:5576–5591

Cölfen H, Antonietti M (2008) Mesocrystals and nonclassical crystallization. Wiley, Chichester

Costodes VCT, Mausse CF, Molala K, Lewis AE (2006) A simple approach for determining particle size enlargement mechanisms in nickel reduction. Int J Miner Process 78:93–100

De Yoreo JJ, Vekilov PG (2003) Principles of crystal nucleation and growth. Rev Mineral Geochem 54:57–93

De Yoreo JJ, Gilbert PUPA, Sommerdijk NAJM, Penn RL, Whitelam S, Joester D, Zhang H, Rimer JD, Navrotsky A, Banfield JF, Wallace AF, Michel FM, Meldrum FC, Cölfen H, Dove PM (2015) Crystallization by particle attachment in synthetic, biogenic, and geologic environments. Science 349, aaa6760

De Yoreo JJ, Sommerdijk NAJM, Dove PM (2017) Nucleation pathways in electrolyte solutions. In: Van Driessche AES, Kellermeier M, Benning LG, Gebauer D (eds) New perspectives on mineral nucleation and growth, Springer, Cham, pp 1–24

Dirksen JA, Benjelloun S, Ring TA (1990) Modelling the precipitation of copper oxalate aggregates. Colloid Polym Sci 268:864–876

Granasy L, Pusztai T, Tegze G, Warren JA, Douglas JF (2005) Growth and form of spherulites. Phys Rev E 72:011605

Hodson ME, Benning LG, Demarchi B, Penkman KEH, Rodriguez-Blanco JD, Schofield PF, Versteegh EAA (2015) Biomineralisation by earthworms – an investigation into the stability and distribution of amorphous calcium carbonate. Geochem Trans 16:1–16

Judat B, Kind M (2004) Morphology and internal structure of barium sulfate – Derivation of a new growth mechanism. J Colloid Interface Sci 269:341–353

Kalsin AM, Fialkowski M, Paszewski M, Smoukov SK, Bishop KJM, Grzybowski BA (2006) Electrostatic self-assembly of binary nanoparticle crystals with a diamond-like lattice. Science 312:420–424

Kim YY, Schenk AS, Ihli J, Kulak AN, Hetherington NBJ, Tang CC, Schmahl WW, Griesshaber E, Hyett G, Meldrum FC (2014) A critical analysis of calcium carbonate mesocrystals. Nat Commun 5:4341

Li D, Nielsen MH, Lee JRI, Frandsen C, Banfield JF, De Yoreo JJ (2012) Direction-specific interactions control crystal growth by oriented attachment. Science 336:1014–1018

Libert S, Gorshkov V, Goia D, Matijević E, Privman V (2003) Model of controlled synthesis of uniform colloid particles: cadmium sulfide. Langmuir 19:10679–10683

Matijevic E (1993) Preparation and properties of uniform size colloids. Chem Mater 5:412–426

Mckenzie JA, Vasconcelos C (2009) Dolomite mountains and the origin of the dolomite rock of which they mainly consist: historical developments and new perspectives. Sedimentology 56:205–219

Nielsen MH, Li D, Zhang H, Aloni S, HanT FC, Seto J, Banfield JF, Cölfen H, De Yoreo JJ (2014) Investigating processes of nanocrystal formation and transformation via liquid cell TEM. Microsc Microanal 20:425–436

Ocana M, Rodriguezclemente R, Serna CJ (1995) Uniform colloidal particles in solution – formation mechanisms. Adv Mater 7:212–216

Park J, Privman V, Matijević E (2001) Model of formation of monodispersed colloids. J Phys Chem B 105:11630–11635

Penn RL, Banfield JF (1998) Imperfect oriented attachment: dislocation generation in defect-free nanocrystals. Science 281:969–971

Penn RL, Banfield JF (1999) Morphology development and crystal growth in nanocrystalline aggregates under hydrothermal conditions: insights from titania. Geochimica Et Cosmochimica Acta 63:1549–1557

Penn RL, Li D, Soltis JA (2017) A perspective on the particle-based crystal growth of ferric oxides, oxyhydroxides, and hydrous oxides. In: Van Driessche AES, Kellermeier M, Benning LG, Gebauer D (eds) New perspectives on mineral nucleation and growth, Springer, Cham, pp 257–274

Pina CM, Becker U, Risthaus P, Bosbach D, Putnis A (1998) Molecular-scale mechanisms of crystal growth in barite. Nature 395:483–486

Pokroy B, Kabalah-Amitai L, Polishchuk I, Devol RT, Blonsky AZ, Sun CY, Marcus MA, Scholl A, Gilbert PUPA (2015) Narrowly distributed crystal orientation in biomineral vaterite. Chem Mater 27:6516–6523

Qi L, Cölfen H, Antonietti M (2000) Crystal design of barium sulfate using double-hydrophilic block copolymers. Angew Chem Int Ed 39:604–607

Rao A, Cölfen H (2017) Mineralization schemes in the living world: mesocrystals. In: Van Driessche AES, Kellermeier M, Benning LG, Gebauer D (eds) New perspectives on mineral nucleation and growth, Springer, Cham, pp 155–184

Sand KK, Rodriguez-Blanco JD, Makovicky E, Benning LG, Stipp SLS (2012) Crystallization of $CaCO_3$ in water-alcohol mixtures: spherulitic growth, polymorph stabilization, and morphology change. Cryst Growth Des 12:842–853

Shtukenberg AG, Punin YO, Gunn E, Kahr B (2012) Spherulites. Chem Rev 112:1805–1838

Soare LC, Bowen P, Lemaitre J, Hofmann H (2006) Precipitation of nanostructured copper oxalate: substructure and growth mechanism. J Phys Chem B 110:17763–17771

Sugimoto T, Khan MM, Muramatsu A (1993) Preparation of monodisperse peanut-type α-Fe2O3 particles from condensed ferric hydroxide gel. Colloids Surf A Physicochem Eng Asp 70: 167–169

Sunagawa I (2005) Crystals: growth, morphology and perfection. Cambridge University Press, Cambridge

Teng HH, Dove PM, De Yoreo JJ (2000) Kinetics of calcite growth: surface processes and relationships to macroscopic rate laws. Geochimica Et Cosmochimica Acta 64:2255–2266

Van Driessche AES, Benning LG, Rodriguez-Blanco JD, Ossorio M, Bots P, García-Ruiz JM (2012) The role and implications of bassanite as a stable precursor phase to gypsum precipitation. Science 335:69–72

Xu AW, Antonietti M, Cölfen H, Fang YP (2006) Uniform hexagonal plates of vaterite $CaCO_3$ mesocrystals formed by biomimetic mineralization. Adv Funct Mater 16:903–908

Yuwono VM, Burrows ND, Soltis JA, Penn RL (2010) Oriented aggregation: formation and transformation of mesocrystal intermediates revealed. J Am Chem Soc 132:2163–2165

Zhang H, De Yoreo JJ, Banfield JF (2014) A unified description of attachment-based crystal growth. ACS Nano 8:6526–6530

Zheng H, Smith RK, Jun YW, Kisielowski C, Dahmen U, Paul Alivisatos A (2009) Observation of single colloidal platinum nanocrystal growth trajectories. Science 324:1309–1312

Zhuang J, Wu H, Yang Y, Cao YC (2008) Controlling colloidal superparticle growth through solvophobic interactions. Angew Chem Int Ed 47:2208–2212